Icosahedral Order, Frustration, and the Glass Transition: Evidence from Time-Dependent Nucleation and Supercooled Liquid Structure Studies

Y. T. Shen, T. H. Kim, A. K. Gangopadhyay, and K. F. Kelton*

Department of Physics, Washington University, St. Louis, Missouri 63130, USA

(Received 23 September 2008; published 6 February 2009)

One explanation for the glass transition is a geometrical frustration owing to the development of non-space-filling short-range order (icosahedral, tetrahedral). However, experimental demonstrations of this are lacking. Here, the first quantitative measurements of the time-dependent nucleation rate in a $Zr_{59}Ti_3Cu_{20}Ni_8Al_{10}$ bulk metallic glass are combined with the first measurements of the evolution of the supercooled liquid structure to near the glass transition temperature to provide strong support for an icosahedral-order-based frustration model for the glass transition in Zr-based glasses.

DOI: 10.1103/PhysRevLett.102.057801 PACS numbers: 61.20.−p, 61.25.Mv, 61.90.+d

The glass transition is arguably one of the most significant problems in condensed matter physics. The dramatic slowing down of the dynamics (structural relaxation, viscous flow) and the loss of ergodicity as the liquid temperature is lowered towards the glass transition temperature (T_g) are poorly understood. While there is general consensus that the dynamics are strongly coupled to the development of local and, perhaps, intermediate-range order in the metastable liquid, the nature of this order is controversial. According to one view the supercooled liquid (metastable liquid below the melting temperature) develops preferred structures that minimize the energy locally [1–4], but which are incompatible with space filling, giving rise to topological or geometric frustration. Frustration models have also been constructed based on the local coordination number [5] and strain [6]. The slowing down of the dynamics is a direct consequence of the frustration. Non-space filling icosahedral short-range order (ISRO) is frequently argued to dominate the local structures of metallic liquids and glasses and to be responsible for topological frustration. This was first suggested by Frank [1] to explain the observed crystal nucleation barrier [1,7,8] and has been supported by a number of subsequent theoretical studies [9,10].

Experimental confirmation of ISRO in liquids and glasses is currently debated. For bulk metallic glasses (BMG), although there are many reports [11] on the structure factor $S(q)$ of the glass, experimental data for the evolution of the liquid structure in the supercooled state do not exist; heterogeneous nucleation of the crystal phase from the container walls hinders such measurements. The usual interpretation of a split second peak in the $S(q)$ of the glasses as evidence for ISRO is questioned, as are the results from reverse Monte Carlo (RMC) analyses [12]. Complementary structural information can be gained from nucleation studies during glass crystallization. Many Zr-based BMGs crystallize to icosahedral quasicrystals, suggesting significant ISRO. Although a number of steady-state nucleation studies in BMG alloys have been reported [13], these are often based on assumptions that may not be justified. *Time-dependent* nucleation rate measurements can be analyzed without such assumptions, and since the rates follow a scaling rule [14], the quality of the data can be assessed. The interfacial mobility, which governs the cluster evolution underlying the nucleation rate, can be measured directly [7], avoiding the extrapolation of high-temperature viscosity data and the use of the Stokes-Einstein equation, which frequently breaks down in the deeply supercooled state [15].

Here we present the first quantitative measurements of the time-dependent nucleation rate in a metallic glass, studying the crystallization of a $Zr_{59}Ti_3Cu_{20}Ni_8Al_{10}$ BMG to an icosahedral quasicrystal (i phase) [16] of the same chemical composition. An extremely small value for the interfacial free energy between the amorphous and i phase, $\sigma_{a\text{-}i}$, is obtained from a detailed analysis of these data. This is much smaller than that between a liquid and a quasicrystal [7,8,17,18], signaling a sharp growth of ISRO with supercooling through the glass transition. This conclusion is confirmed by our direct measurements of the evolution of the local structure of the liquid in the deeply supercooled and amorphous states, based on a RMC analysis of liquid diffraction data. These results from two very different experiments provide the strongest experimental demonstration to date that ISRO dominates the structures of both the liquid and the glass and provide strong support for an ISRO-based frustration model [3,4] for the glass transition in this and, possibly, other Zr-based metallic glasses.

According to the classical nucleation theory [7], random fluctuations in the liquid produce an ensemble of small clusters having the structure of the ordered phase. However, only those clusters exceeding a critical size (n^* atoms) can *nucleate and grow*. For liquids, the steady-state nucleation rate for such clusters, I^s, is generally estimated from the maximum supercooling temperature before crystallization [7,17]. Nucleation and growth occur simultaneously, however, introducing some uncertainty in the values obtained. In silicate glasses it has been demonstrated that a two-step annealing treatment can be used to obtain

quantitative steady state and time-dependent nucleation data [19]; the first two-step measurements of nucleation in a metallic glass are reported here. Glasses are first annealed at a nucleation temperature T_N, where the nucleation rate is high but the growth rate is low, to produce a population of nuclei. A subsequent anneal at a higher temperature, T_G, where the nucleation rate is low but the growth rate is fast, allows these nuclei to grow to observable size. The rate of production of clusters larger than $n^*(T_G)$ is then directly obtained [19–21].

Samples of $Zr_{59}Ti_3Cu_{20}Ni_8Al_{10}$ were prepared as described elsewhere [22]. Although amorphous ingots can be made easily, for convenience, 30–50 μm thick amorphous ribbons were used in this study. For the nucleation anneal, the ribbons were wrapped in an Al foil and annealed between 385 °C–400 °C ($T_g = 382$ °C, $T_{\text{cryst}} = 451$ °C [16]) for various lengths of times in a temperature controlled (± 0.5 °C) lead-tin bath. A growth treatment of 2 min at 430 °C was used. X-ray and TEM diffraction studies confirmed that only the i phase was formed during these anneals. The number of i phase grains produced after the nucleation and growth treatments were counted manually from transmission electron microscopy images. The number of i phase grains per unit volume N_v is shown as a function of annealing time t and nucleation temperature T_N in Fig. 1(a). Corrections to N_v for sample thickness were made using a modified Saltykov method [23].

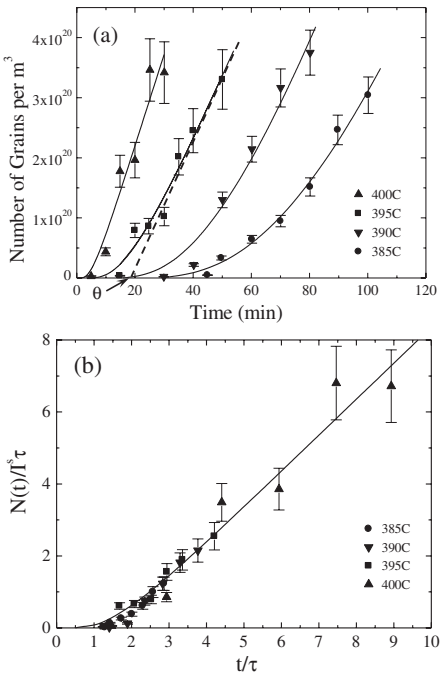

FIG. 1. (a) Number of quasicrystal grains per unit volume N_v as a function of annealing time at the nucleation temperature T_N. The growth temperature was 430 °C. The slope of N_v versus t equals I^s at long annealing times. The induction time θ is obtained by extrapolating N_v in the steady-state regime to the time axis (illustrated by the dashed line for the 395 °C data). (b) Fit to scaling relation predicted from classical theory of nucleation [Eq. (1)].

The nucleation rate (dN_v/dt) is initially low and approaches the constant slope steady-state value, I^s, only after long annealing times [shown by the dashed line in Fig. 1(a)]. This time-dependent nucleation [20] reflects an evolution of the crystal cluster size distribution inherited in the glass during the quench to the steady-state distribution at the annealing temperature T_N. The characteristic time that describes this evolution is the transient time τ [14,20], obtained from the induction time θ ($\tau = 6\theta/\pi^2$), which is given by the intercept of the slope of a $N(t)$ versus t plot, extrapolated from the steady-state regime to the time axis [dashed line in Fig. 1(a)]. The classical theory of nucleation [7,14] predicts that $N(t)$ should follow a scaling relation:

$$\frac{N(t)}{I^s\tau} = \frac{t}{\tau} - \frac{\pi^2}{6} - 2\sum_{n=1}^{\infty}\frac{(-1)^n}{n^2}\exp\left(-\frac{n^2 t}{\tau}\right). \quad (1)$$

The observed excellent agreement of the data to Eq. (1), shown in Fig. 1(b), demonstrates the high quality of the nucleation data. They can be quantitatively analyzed to provide accurate estimates of the interfacial free energy. A distinct advantage of time-dependent data is that the induction time provides a direct measure of the appropriate interfacial attachment frequency, obviating the need for extrapolations of high-temperature viscosity data and the use of the Stokes-Einstein equation to extract a jump mobility, which can fail at deep supercoolings [15].

From the classical theory [7],

$$I^s\theta_{n^*(T_N)} = A^*\exp\left[-\frac{16\pi}{3k_B}\frac{\sigma_{a-i}^3}{T(\Delta G_v)^2}\right]$$
$$\text{or} \quad \ln(I^s\theta_{n^*(T_N)}) = \ln(A^*) - \left(\frac{16\pi}{3k_BT(\Delta G_v)^2}\right)\sigma_{a\text{-}i}^3, \quad (2)$$

where ΔG_v is the driving free energy per unit volume for crystallization, k_B is Boltzmann's constant, and A^* is approximately constant. The driving free energy ΔG_v was calculated [7] from the enthalpy of transformation between the supercooled liquid and the i phase [ΔH (703 K) = 1427 J/mol] and the measured specific heat difference $\Delta c_p^{a\text{-}i} = c_p^a - c_p^i = -361.87 + 0.971\,T - 6.080 \times 10^{-4}\,T^2$ (J/mol K) between the amorphous and crystal phases, measured by differential scanning calorimetry (DSC). Since the metastable liquidus temperature for the i phase is not known, conservative bounds were placed. The lower bound was taken to be 459 °C, corresponding to the termination temperature for the primary crystallization peak in DSC scans. An upper bound of 527 °C corresponded to the first exothermic event observed during free cooling of the liquid in electrostatic levitation [22] and the complete crystallization of the glass in DSC scans. Note that the induction time needed in Eq. (2) is for the critical size at the nucleation temperature $\theta_{n^*(T_N)}$; the measured induction time is for the critical size at the growth temperature, $\theta_{n^*(T_G)}$. $\theta_{n^*(T_N)}$ may be obtained from the measured data using [24]

$$\frac{\theta_{n^*(T_G)}}{\theta_{n^*(T_N)}} = \frac{6}{\pi^2}\left(x + \ln x + \ln\frac{6W^*}{k_B T} + \varsigma - 1\right), \qquad (3)$$

where $x = [n^*(T_G)/n^*(T_N)]^{1/3} - 1$, $n^*(T_N)$ and $n^*(T_G)$ are the critical sizes at the nucleation and growth temperatures, respectively, and ζ is Euler's constant (0.5772); W^* is the work for critical cluster formation calculated at T_N and $n^* = (32\pi/3\bar{v})(\sigma_{a-i}/|\Delta G_v|)^3$.

As shown in Fig. 2, a plot of $\ln(I^s\theta_{n^*(T_N)})$ versus $(16\pi/3k_BT\Delta G_v^2)$ gives the expected straight line [Eq. (2)]; σ_{a-i} is the cube root of the slope of this line. Since σ_{a-i} is required for the induction time correction [Eq. (3)], it was first estimated using $\theta_{n^*(T_G)}$. The values for σ_{a-i} and $\theta_{n^*(T_N)}$ were then refined by iteration until convergence, generally within less than five iterations. The final value of the interfacial free energy obtained is 0.01 ± 0.004 J/m^2 (error primarily reflects the uncertainty in the metastable liquidus temperature). Such a small interfacial free energy, almost an order of magnitude smaller than the values obtained between a supercooled liquid and a quasicrystal [7,8,17,18], implies very strong ISRO in the glass.

To investigate this further, x-ray diffraction measurements were made on electrostatically levitated, nearly spherical (2.3–2.5 mm diameter), droplets of supercooled liquid and glass at the Advanced Photon Source (APS, μ-CAT 6ID-D) using 125 keV x rays, as described elsewhere [17,25]. The pair correlation function, $g(r)$, computed from the measured $S(q)$ is shown in Fig. 3. Structural models for the liquids were obtained from RMC [12] simulations on 5000 atoms in a cube of side $L = 45.86$ Å, assuming periodic boundary conditions. The atomic number densities ρ_0 used were 0.0523 (27 °C), 0.0518 (700 °C), 0.0511 (900 °C), 0.0509 (1000 °C), 0.0506 (1100 °C), 0.0503 (1200 °C), obtained from the measured liquid densities (see [26]); the density (0.0522) at T_g (382 °C) was obtained by extrapolation. The cutoff distance was 2.1 Å to prevent overlapping of the atoms. As shown in Fig. 3, the calculated $g(r)$ is in good agreement with the experimental data.

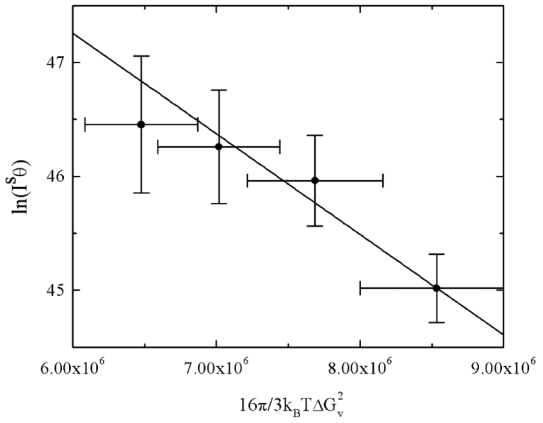

FIG. 2. Plot of the log of the product of the experimentally measured steady-state nucleation rate and the induction time as a function of the inverse driving free energy and temperature for i phase nucleation in a $Zr_{59}Ti_3Cu_{20}Ni_8Al_{10}$ metallic glass. The straight line is a best fit to the data points. The vertical error bars reflect the experimental uncertainty in measurements of the induction time and steady-state nucleation rates. The horizontal ones reflect the uncertainty in the quasicrystal metastable liquidus temperature (see text) as well as that in the specific heat measurements of the supercooled liquid near the glass transition.

The topologies of the RMC generated structures were analyzed in terms of their bond-orientational order (BOO) parameters [2] and Honeycutt-Andersen (HA) indices [27]. As shown in Fig. 4(a), only the Q_6 BOO, corresponding to ISRO, showed a significant monotonic increase with supercooling, which was also observed in earlier molecular dynamics simulation studies of liquids interacting via a Lennard-Jones potential [2].

In agreement with the BOO results, the densities of the HA indices reflecting ISRO (1551) and distorted ISRO (1541 and 1431) are the largest and increase with supercooling [Fig. 4(b)]. The rate of change of the intensity of the HA index 1551 slows down dramatically near the glass transition, reflecting configurational freezing. A small fraction of the liquid is characterized by crystal-type order (HA index 1661 for bcc and 1421 and 1422 for fcc and hcp, for example), but the intensities of these indices (not shown here) remain constant or decrease slightly with supercooling. Since it was not possible to obtain liquid structure data very close to the glass transition temperature (382 °C [16]) due to crystallization, the corresponding HA index 1551 intensity [square symbol in Fig. 4(b)] was obtained from an $S(q)$ that was computed [28] from the structure factor at room temperature. While this may influence the precise position of the dashed line in Fig. 4(b), the main conclusion is unaffected; the evolution of the order slows significantly near T_g. Both the BOO and the HA metrics, therefore, indicate a significant increase in the ISRO in the supercooled liquid down to T_g, in agreement with the results of the nucleation measurements.

In conclusion, these first quantitative time-dependent nucleation measurements in a metallic glass indicate that

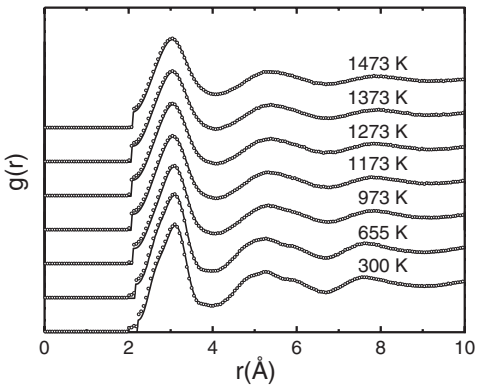

FIG. 3. The $g(r)$ computed from the experimental $S(q)$ (circles) and the RMC fits (solid lines); the data were sparsely plotted to show the quality of the fits.

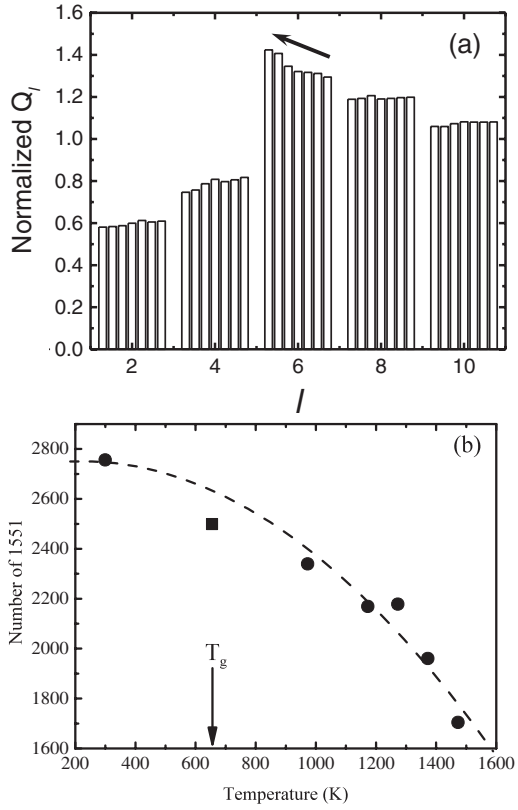

FIG. 4. (a) A normalized BOO analysis of $Zr_{59}Ti_3Cu_{20}Ni_8Al_{10}$ alloy at various temperatures. The arrow indicates the direction of decreasing temperature. (b) The intensity of the 1551 Honeycutt-Andersen index (characteristic of ISRO) as a function of liquid temperature. The dashed line is a polynomial fit.

the interfacial free energy between the icosahedral quasicrystal phase and the glass in $Zr_{59}Ti_3Cu_{20}Ni_8Al_{10}$ is extremely small. Taken with the results of the analysis of the first x-ray diffraction data of the supercooled liquid and glass, a clear case is made for dominant ISRO in this liquid and glass. The ISRO increases dramatically with supercooling to the glass transition, providing the strongest experimental evidence to date of the connection between ISRO and the frustration underlying the glass transition in this and related glasses. Further, it indicates that ISRO can play a central role in glass formation in Zr-based bulk metallic glasses. The growth of ISRO in the supercooled liquid raises the nucleation barrier for the formation of crystal phases and increases the viscosity of the liquid [4,13], making it easier to form the glass.

We thank R. W. Hyers, S. M. Canepari, and J. R. Rogers for allowing us to use their unpublished density data and A. I. Goldman and J. R. Rogers for help in data acquisition. The work at Washington University was partially supported by the National Science Foundation under Grant No. DMR-0606065 and by NASA under Contract No. NNM04AA016. MUCAT is supported by the U.S. Department of Energy, Office of Science under Contract No. W-7405-Eng-82. Use of the Advanced Photon Source is supported by the U.S. Department of Energy, Basic Energy Sciences, Office of Science, under Contract No. W-31-109-Eng-38.

*Corresponding author.
kfk@wuphys.wustl.edu

[1] F. C. Frank, Proc. R. Soc. A **215**, 43 (1952).
[2] P. J. Steinhardt, D. R. Nelson, and M. Ronchetti, Phys. Rev. Lett. **47**, 1297 (1981); Phys. Rev. B **28**, 784 (1983).
[3] G. Tarjus *et al.*, J. Phys. Condens. Matter **17**, R1143 (2005).
[4] H. Tanaka, J. Phys. Condens. Matter **15**, L491 (2003).
[5] D. B. Miracle, Nature Mater. **3**, 697 (2004).
[6] T. Egami and D. Srolovitz, J. Phys. F **12**, 2141 (1982); T. Egami, Phys. Rev. B **76**, 024203 (2007).
[7] K. F. Kelton, in *Solid State Physics*, edited by H. Ehrenreich and D. Turnbull (Academic, Boston, 1991), Vol. 45, p. 75.
[8] D. Holland-Moritz *et al.*, Acta Mater. **46**, 1601 (1998); G. W. Lee *et al.*, Phys. Rev. B **72**, 174107 (2005).
[9] J. L. Finney, Proc. R. Soc. A **319**, 479 (1970); **319**, 495 (1970); J. L. Finney, Nature (London) **266**, 309 (1977); H. W. Sheng *et al.*, Nature (London) **439**, 419 (2006).
[10] D. R. Nelson and F. Spaepen, in *Solid State Physics*, edited by H. Ehrenreich and D. Turnbull (Academic, Boston, 1989), Vol. 42, p. 1.
[11] N. Mattern *et al.*, Acta Mater. **50**, 305 (2002).
[12] D. A. Keen and R. L. McGreevy, Nature (London) **344**, 423 (1990); R. L. McGreevy, J. Phys. Condens. Matter **3**, F9 (1991).
[13] S. Mukherjee *et al.*, Phys. Rev. Lett. **94**, 245501 (2005); B. A. Legg, J. Schroers, and R. Busch, Acta Mater. **55**, 1109 (2007).
[14] D. Kashchiev, Surf. Sci. **14**, 209 (1969).
[15] U. Geyer *et al.*, Phys. Rev. Lett. **75**, 2364 (1995).
[16] L. Q. Xing *et al.*, Appl. Phys. Lett. **77**, 1970 (2000).
[17] K. F. Kelton *et al.*, Phys. Rev. Lett. **90**, 195504 (2003).
[18] D. Holland-Moritz, D. M. Herlach, and K. Urban, Phys. Rev. Lett. **71**, 1196 (1993).
[19] P. F. James, Phys. Chem. Glasses **15**, 95 (1974).
[20] K. F. Kelton and A. L. Greer, Phys. Rev. B **38**, 10 089 (1988); K. F. Kelton, A. L. Greer, and C. V. Thompson, J. Chem. Phys. **79**, 6261 (1983); A. L. Greer and K. F. Kelton, J. Am. Ceram. Soc. **74**, 1015 (1991).
[21] A. M. Kalinina, V. N. Filipovich, and V. M. Fokin, J. Non-Cryst. Solids **38–39**, 723 (1980); K. F. Kelton and A. L. Greer, in *Rapidly Quenched Metals*, edited by S. Steeb and H. Warlimont (North-Holland, Amsterdam, 1985), p. 223.
[22] T. H. Kim *et al.*, Appl. Phys. Lett. **87**, 251924 (2005).
[23] D. Jensen, J. Phys. D **28**, 549 (1995).
[24] V. A. Shneidman and M. C. Weinberg, J. Chem. Phys. **97**, 3621 (1992).
[25] A. K. Gangopadhyay *et al.*, Rev. Sci. Instrum. **76**, 073901 (2005).
[26] R. C. Bradshaw *et al.*, Rev. Sci. Instrum. **76**, 125108 (2005).
[27] J. D. Honeycutt and H. C. Andersen, J. Phys. Chem. **91**, 4950 (1987).
[28] N. Mattern *et al.*, J. Non-Cryst. Solids **345–346**, 758 (2004).